DELFT UNIVERSITY OF TECHNOLOGY

REPORT 18-05

Efficient and robust Schur complement approximations in the augmented Lagrangian preconditioner for high Reynolds number laminar flows

X. He and C. Vuik

ISSN 1389-6520

Reports of the Delft Institute of Applied Mathematics

Delft 2018

Abstract

This report introduces three new Schur complement approximations for the augmented Lagrangian preconditioner based on the method proposed by He, Vuik and Klaij [*SIAM J. Sci. Comput.,* 40 (2018), pp. A1362-A1385]. The incompressible Navier-Stokes equations discretized by a stabilized finite element method are utilized to evaluate these new approximations of the Schur complement. A wide range of numerical experiments in the laminar context determines the most efficient Schur complement approximation and investigates the effect of the Reynolds number, mesh anisotropy and refinement on the optimal choice. Furthermore, the advantage over the traditional Schur complement approximation is exhibited.

Mathematics subject classification: 65F10, 65F08.

Key words: incompressible Navier-Stokes equations, stabilized finite element method, block structured preconditioners, Schur complement approximations, augmented Lagrangian preconditioner.

1 Introduction

Block structured preconditioners [11,30,31] are often utilised to accelerate the convergence of the Krylov subspace solvers for the saddle point systems arising from the incompressible Navier-Stokes equations. The key to attain efficient block structured preconditioners is the spectrally equivalent and numerically cheap approximation of the Schur complement [2,29]. There exist several state-of-the-art approximations of the Schur complement, e.g. the least-square commutator (LSC) [8,9], pressure convection-diffusion (PCD) operator [21,32] and the approximations from the block structured SIMPLE(R) [24,25,33] and augmented Lagrangian (AL) preconditioner [3, 15] etc. Among them, the AL preconditioner exhibits attractive features with stable finite element methods (FEM) used for the discretization, e.g. the purely algebraic and simple construction of the Schur complement approximation and robustness with respect to the mesh refinement and Reynolds number, at least for academic benchmarks. Motivated by these advantages, the further extension to the context of finite volume method (FVM) [17] and the modified variant [4] with reduced computational complexities are promoted. Recently, the authors of this paper propose a new variant of the AL preconditioner [18] for the Reynolds-Averaged Navier-Stokes (RANS) equations discretized by a stabilized FVM, which are widely used to model turbulent flows in industrial computational fluid dynamic (CFD) applications.

Although the solution procedure of the RANS equations consists of solving a sequence of linear systems in saddle point form, the research in [18] shows that the straightforward application of the AL preconditioner leads to a very slow convergence of the Krylov subspace solvers. The challenges encountered in the turbulent calculations [12,28,34] are inevitable factors which could cause the breakdown of the AL preconditioner, including the high Reynolds number, high-aspect ratio cells near the very thin boundary layer and the significant variation in the value of viscosity due to the presence of the eddy-viscosity.

To overcome these challenges, an alternative method to approximate the Schur complement for the AL preconditioner is introduced in [18], which leads to a new variant of the AL preconditioner. This new method approximates the Schur complement through its inverse form and facilitates the utilization of the existing Schur complement approximations. Among the available candidates, the Schur complement approximation from the SIMPLE preconditioner [22, 24] is chosen and substituted into the inverse Schur complement approximation for the AL preconditioner. This choice is motivated from the notion that it reduces to a scaled Laplacian matrix [22, 24] with the considered FVM and its promising efficiency on the turbulent applications of the maritime industry [23, 24]. Consequently, the so-arising new variant of the AL preconditioner reduces the number of Krylov subspace iterations by a factor up to 36 compared to the original one [18].

Since the new method to approximate the Schur complement for the AL preconditioner use the existing Schur complement approximations, the following questions straightforwardly raise. Does the utilization of other existing Schur complement approximations deliver a better performance than that from the SIMPLE preconditioner? If so, which Schur complement approximation is the most efficient one? Does the optimal choice depend on the test problem and parameters arising from the physics and discretization, e.g. the Reynolds number and grid size? To answer these questions, in this paper we utilize the existing Schur complement approximations not only from the SIMPLE preconditioner but also from the LSC and PCD operators to construct the new Schur complement approximation in the AL preconditioner. Moreover, extensive comparisons between the considered Schur complement approximations are carried out on a wide range of numerical experiments to evaluate the effect of the Reynolds number, mesh anisotropy and refinement on the optimal choice. These numerical evaluations are considered in the context of laminar flows, which is motivated by the expectation that the obtained results can provide a fundamental guideline for the more complicated turbulent flow calculations.

In this paper we use the mixed FEM which does not uniformly satisfy a discrete inf-sup condition [11] to discretize the Navier-Stokes equations governing laminar flows, which is chosen by the following considerations. First, the existing Schur complement approximations are originally designed with finite element methods used for discretization. Therefore, it is expected to apply the new Schur complement approximation for the AL preconditioner in the FEM context. In addition, this closes a gap in the application of the new Schur complement approximation. Second, both the stabilized FEM [11] and FVM [12] lead to saddle point system with a nonzero $(2, 2)$ block which arises from the pressure stabilization. Thanks to this similarity, a minor adaption is required to extend the new variant of the AL preconditioner from the stabilized FVM to the stabilized FEM. Finally, the utilization of stabilized FVM degrades the generality to some extent since the Schur complement approximation in the SIMPLE preconditioner reduces to a special formation [22, 24]. However, this special formation can not be obtained with other stabilization and discretization methods. Using stabilized FEM, all Schur complement approximations considered in this paper are expressed in their defined manners, including that from the SIMPLE preconditioner. In this way, a convincing evaluation of the novel Schur complement approximation for the AL preconditioner can be expected.

The structure of this paper is given as follows. The saddle point system arising from the incompressible Navier-Stokes equations is introduced in Section 2, followed by a brief survey of the existing approximations of the Schur complement. Section 3 illustrates the method using these existing Schur complement approximations to construct the new approximation of the Schur complement in the AL preconditioner. Section 4 includes numerical results on varying laminar benchmarks. Conclusions and future work are outlined in Section 5.

2 Problem formulation

In this paper we consider the steady, laminar and incompressible Navier-Stokes equations as follows

$$\begin{aligned} -\nu\Delta\mathbf{u} + (\mathbf{u}\cdot\nabla)\mathbf{u} + \nabla p = \mathbf{f} \quad &\text{on } \Omega, \\ \nabla\cdot\mathbf{u} = 0 \quad &\text{on } \Omega. \end{aligned} \tag{1}$$

Here $\mathbf{u}$ is the velocity, p is the pressure, the positive coefficient ν is the kinematic viscosity and $\mathbf{f}$ is a given force field. Ω is a 2D or 3D bounded and connected domain with the boundary $\partial\Omega$. On the boundaries of the computational domain, either the Dirichlet boundary condition $\mathbf{u} = \mathbf{g}$ or Neumann boundary condition $\nu\frac{\partial\mathbf{u}}{\partial\mathbf{n}} - \mathbf{n}p = 0$ is imposed, where $\mathbf{n}$ denotes the outward-pointing unit normal to the boundary.

After the Picard linearization and FEM discretization [11], the incompressible Navier-Stokes equations convert to the following linear system in saddle-point form

$$\begin{bmatrix} A & B^T \\ B & -\frac{1}{\nu}C \end{bmatrix} \begin{bmatrix} \mathbf{u} \\ p \end{bmatrix} = \begin{bmatrix} \mathbf{f} \\ g \end{bmatrix} \quad \text{with} \quad \mathcal{A} := \begin{bmatrix} A & B^T \\ B & -\frac{1}{\nu}C \end{bmatrix}, \tag{2}$$

where the matrices B and B^T correspond to the divergence and gradient operators, respectively. Picard linearization leads to the matrix A in block diagonal structure, and each diagonal block corresponds to the convection-diffusion operator. Due to the presence of the convective term, A is not symmetric.

For the finite element discretization satisfying the LBB ('inf-sup') stability condition [11], no pressure stabilization is required and $C = 0$ is taken. When LBB unstable finite elements are applied, the nonzero matrix C corresponds to a stabilization operator. Based on the motivations presented in the introduction, in this paper we use the Q_1-Q_1 mixed finite element approximation where the equal first-order discrete velocities and pressure are specified on a common set of nodes. Among the available stabilization methods [1, 5–7, 13, 20] specified for the Q_1-Q_1 discretization, we choose the approach introduced in [7]. The main motivation is that there is no stabilization parameter required in the following operator

$$C^{(proj)}(p_h, q_h) = (p_h - \Pi_0 p_h, q_h - \Pi_0 q_h), \tag{3}$$

where Π_0 is the L^2 projection from the pressure approximation space into the space P_0 of the piecewise constant basis function. This projection is defined locally: $\Pi_0 p_h$ is a constant

function in each element $\square_k \in T_h$. It is determined simply by the following local averaging

$$\Pi_0 p_h|_{\square_k} = \frac{1}{|\square_k|}\int_{\square_k} p_h, \quad \text{for all } \square_k \in T_h, \tag{4}$$

where $|\square_k|$ is the area of element k. Due to the locality as illustrated by equation (4), the stabilization matrix C can be assembled from the contribution matrices on macroelements in the same way as assembling a standard finite element mass matrix. Taking the 2D rectangular grid as an example, the 4×4 macroelement contribution matrix $C^{(macro)}$ is given by

$$C^{(macro)} = M^{(macro)} - qq^T|\square_k|, \tag{5}$$

where $M^{(macro)}$ is the 4×4 macroelement mass matrix for the bilinear discretization and $q = [1/4, 1/4, 1/4, 1/4]^T$ is the local averaging operator. The null space of the macroelement matrix $C^{(macro)}$ and assembled stabilization matrix C consist of constant vector, see [7, 11] for more details.

Block structured preconditioners are meant to accelerate the convergence of the Krylov subspace solvers for saddle point systems as (2). They are based on the block $\mathcal{LDU}$ decomposition of the coefficient matrix given by

$$\mathcal{A} = \mathcal{LDU} = \begin{bmatrix} A & B^T \\ B & -\frac{1}{\nu}C \end{bmatrix} = \begin{bmatrix} I_1 & O \\ BA^{-1} & I_2 \end{bmatrix} \begin{bmatrix} A & O \\ O & S \end{bmatrix} \begin{bmatrix} I_1 & A^{-1}B^T \\ O & I_2 \end{bmatrix}, \tag{6}$$

where $S = -(\nu^{-1}C + BA^{-1}B^T)$ is the so-called Schur complement. A combination of this block factorization with a suitable approximation of the Schur complement is utilised to successfully design the block structured preconditioners, which are given as follows

$$\mathcal{P}_F = \begin{bmatrix} A & O \\ B & \widetilde{S} \end{bmatrix} \begin{bmatrix} I_1 & \widetilde{A}^{-1}B^T \\ O & I_2 \end{bmatrix}, \tag{7}$$

$$\mathcal{P}_L = \begin{bmatrix} A & O \\ B & \widetilde{S} \end{bmatrix}, \qquad \mathcal{P}_U = \begin{bmatrix} A & B^T \\ O & \widetilde{S} \end{bmatrix}. \tag{8}$$

Multiplying the $\mathcal{LD}$ and $\mathcal{DU}$ factors of (6) results in the block lower- and upper-triangular preconditioners $\mathcal{P}_L$ and $\mathcal{P}_U$, respectively. Preconditioner $\mathcal{P}_F$ is based on the multiplication of the $\mathcal{LDU}$ factors. The term $\widetilde{A}^{-1}$ denotes some approximation of the inverse action of A, which is given either in an explicit form or implicitly defined via an iterative solution method with a proper stopping tolerance.

It is not practical to explicitly form the exact Schur complement due to the action of A^{-1}, typically when the size is large. This implies that the most challenging task is to find the spectrally equivalent and numerically cheap approximation of the Schur complement, which is denoted by $\widetilde{S}$ in (7) and (8). As follows we briefly introduce several state-of-the-art Schur complement approximations which are utilised to construct the new approximation of the Schur complement for the AL preconditioner. We refer for more details of the Schur complement approximation to the surveys [2, 29–31] and the books [11, 27].

In the following illustration, we use the notation p to indicate the operators defined on the pressure space and the notation u for the operators defined on the velocity space.

(1) **The pressure convection-diffusion operator $\widetilde{S}_{PCD}$.**

This approximation, denoted by $\widetilde{S}_{PCD}$, is proposed by Kay et al [21] and defined as

$$\widetilde{S}_{PCD} = -L_p A_p^{-1} M_p, \tag{9}$$

where M_p is the pressure mass matrix, and A_p and L_p are the discrete pressure convection-diffusion and Laplacian operators, respectively. Although the PCD Schur complement approximation (9) is originally proposed for stable finite element methods, it is straightforwardly applicable for the discretizations needing a stabilization term, e.g. the Q_1-Q_1 pair. For more details about this extension we refer to [11]. On the other hand, this approximation requires users to provide the discrete operators A_p and L_p and preset some artificial pressure boundary conditions on them. The boundary conditions could strongly effect the performance so appropriate ones should be carefully selected based on the problem characteristic [10, 19]. Applying the PCD Schur complement approximation involves the action of a Poisson solve, a mass matrix solve and a matrix-vector product with the matrix A_p.

(2) **The least-square commutator $\widetilde{S}_{LSC}$.**

Elman et al [8] originally propose this method for stable finite element discretizations and then extend it to alternatives [9] that require stabilization. For system (2) with a nonzero stabilization operator C, the LSC Schur complement approximation $\widetilde{S}_{LSC}$ is defined as

$$\widetilde{S}_{LSC} = -(B\widehat{M}_u^{-1}B^T + C_1)(B\widehat{M}_u^{-1}A\widehat{M}_u^{-1}B^T + C_2)^{-1}(B\widehat{M}_u^{-1}B^T + C_1), \tag{10}$$

where $\widehat{M}_u$ denotes the diagonal approximation of the velocity mass matrix M_u, i.e. $\widehat{M}_u = \mathrm{diag}(M_u)$. Given the stabilization matrix C assembled from the macroelement contribution matrix $C^{(macro)}$ (5), the contribution matrices $C_1^{(macro)}$ and $C_2^{(macro)}$ for the associated stabilization matrices C_1 and C_2 are introduced by

$$C_1^{(macro)} = \frac{1}{|\square_k|} \cdot C^{(macro)}, \quad C_2^{(macro)} = \frac{\nu}{|\square_k|^2} \cdot C^{(macro)}, \tag{11}$$

where ν denotes the viscosity parameter. For the derivation of $C_1^{(macro)}$ and $C_2^{(macro)}$ we refer to [9]. The implementation of the LSC Schur complement approximation does not require any artificial boundary condition and consists of one matrix-vector product with the middle term in (10) and two solves with the other term. When the LSC Schur complement approximation is applied to stable finite element discretizations, the matrices C_1 and C_2 are set to zero in (10).

(3) **The approximation $\widetilde{S}_{SIMPLE}$ from the SIMPLE preconditioner.**

SIMPLE (Semi-Implicit Pressure Linked Equation) is used by Patanker [28] as an iterative method to solve the Navier-Stokes problem. The scheme belongs to the

class of basic iterative methods and exhibits slow convergence. Vuik et al [25, 33] use SIMPLE as a preconditioner in a Krylov subspace method, achieving in this way, a much faster convergence. Regarding the Schur complement $S = -(\nu^{-1}C + BA^{-1}B^T)$ of system (2), the SIMPLE preconditioner approximates A by its diagonal, i.e. $\mathrm{diag}(A)$, and obtains the approximation $\widetilde{S}_{SIMPLE}$ as

$$\widetilde{S}_{SIMPLE} = -(\nu^{-1}C + B\mathrm{diag}(A)^{-1}B^T). \tag{12}$$

Substituting $\widetilde{S}_{SIMPLE}$ and $\widetilde{A}^{-1} = \mathrm{diag}(A)^{-1}$ into (7) leads to the so-called SIMPLE preconditioner. For stable finite element discretizations, $C = 0$ is set in system (2) and correspondingly in the Schur complement approximation (12). The easy implementation and promising performance on the complicated maritime problems [23, 24] make the SIMPLE preconditioner and its variants attractive in real world applications.

The main goal of this paper is to utilise the above mentioned Schur complement approximations to construct a new approximation of the Schur complement in the AL preconditioner, with more details presented in the next section. Theoretical analysis and numerical evaluation of the above Schur complement approximations fall out of the scope of this work and we refer to [11, 16, 31] for more results. Here we summarize the key differences. $\widetilde{S}_{PCD}$ requires the construction of additional matrices on the pressure space while $\widetilde{S}_{LSC}$ and $\widetilde{S}_{SIMPLE}$ rely on matrices which could be easily generated or are readily available. As seen from $\widetilde{S}_{LSC}$, the stabilization terms $C_1^{(macro)}$ and $C_2^{(macro)}$ are easily obtained by substituting the available term $C^{(macro)}$ into (11). On the other hand, $\widetilde{S}_{PCD}$ easily extends to the stabilized elements and a minor adaption is required by $\widetilde{S}_{SIMPLE}$ for this extension. However, $\widetilde{S}_{LSC}$ does not immediately apply and needs appropriate stabilization terms C_1 and C_2. We further note that boundary conditions for the pressure unknowns, which have few physical meanings, have to be considered for L_p and A_p in $\widetilde{S}_{PCD}$. What boundary conditions work best with a specific type of problem is usually based on experimental knowledge [10, 19].

3 Augmented Lagrangian preconditioner

The focus of this section is the new method to approximate the Schur complement in the augmented Lagrangian (AL) preconditioner. In the following, we first briefly recall the AL preconditioner and then introduce the new method followed by a comparison with the old one.

The motivation of applying the AL preconditioner is to circumvent the challenge on finding the efficient approximation of the Schur complement S for the original system (2), c.f., [3, 4]. To apply the AL preconditioner, the original system (2) is transformed into an equivalent one with the same solution [4, 17], which is of the form

$$\begin{bmatrix} A_\gamma & B_\gamma^T \\ B & -\frac{1}{\nu}C \end{bmatrix} \begin{bmatrix} \mathbf{u} \\ p \end{bmatrix} = \begin{bmatrix} \mathbf{f}_\gamma \\ g \end{bmatrix} \quad \text{with} \quad \mathcal{A}_\gamma := \begin{bmatrix} A_\gamma & B_\gamma^T \\ B & -\frac{1}{\nu}C \end{bmatrix}, \tag{13}$$

where $A_\gamma = A + \gamma B^T W^{-1} B$, $B_\gamma^T = B^T - \gamma/\nu B^T W^{-1} C$ and $\mathbf{f}_\gamma = \mathbf{f} + \gamma B^T W^{-1} g$. This transformation is obtained by multiplying $\gamma B^T W^{-1}$ on both sides of the second row of system (2) and adding the resulting equation to the first one. Clearly, the transformed system (13) has the same solution as system (2) for any value of γ and any non-singular matrix W. The Schur complement of the transformed system (13) is $S_\gamma = -(\nu^{-1} C + B A_\gamma^{-1} B_\gamma^T)$.

The AL preconditioner is applied for the equivalent system (13), which is to be solved. Using the block $\mathcal{D}U$ decomposition of $\mathcal{A}_\gamma$, the ideal AL preconditioner $\mathcal{P}_{IAL}$ and its variant, i.e. the modified AL preconditioner $\mathcal{P}_{MAL}$, are given by

$$\mathcal{P}_{IAL} = \begin{bmatrix} A_\gamma & B_\gamma^T \\ O & \widetilde{S}_\gamma \end{bmatrix} \quad \text{and} \quad \mathcal{P}_{MAL} = \begin{bmatrix} \widetilde{A}_\gamma & B_\gamma^T \\ O & \widetilde{S}_\gamma \end{bmatrix}, \tag{14}$$

where $\widetilde{S}_\gamma$ and $\widetilde{A}_\gamma$ denote the approximations of S_γ and A_γ, respectively.

First we consider the approximation $\widetilde{A}_\gamma$. Given the original pivot matrix $A = \begin{bmatrix} A_1 & O \\ O & A_1 \end{bmatrix}$ and the divergence matrix $B = \begin{bmatrix} B_1 & B_2 \end{bmatrix}$ in the 2D case, the transformed pivot matrix $A_\gamma = A + \gamma B^T W^{-1} B$ can be written as

$$A_\gamma = \begin{bmatrix} A_1 + \gamma B_1^T W^{-1} B_1 & \gamma B_1^T W^{-1} B_2 \\ \gamma B_2^T W^{-1} B_1 & A_1 + \gamma B_2^T W^{-1} B_2 \end{bmatrix}.$$

Contrary to $\mathcal{P}_{IAL}$, $\mathcal{P}_{MAL}$ approximates A_γ by its block upper-triangular part, i.e. $\widetilde{A}_\gamma$ with a zero (2,1) block, such that the difficulty of solving the systems with A_γ is avoided [4]. When applying $\mathcal{P}_{MAL}$ one needs to solve the sub-systems with the diagonal blocks of A_γ, i.e. $A_1 + \gamma B_1^T W^{-1} B_1$ and $A_1 + \gamma B_2^T W^{-1} B_2$, which do not contain the coupling between two components of the velocity so that it is much easier to solve, compared to A_γ involved in $\mathcal{P}_{IAL}$. This advantage motivates us to choose $\mathcal{P}_{MAL}$ in this paper.

3.1 New Schur approximation in the AL preconditioner

Finding an effective approximation of the Schur complement S_γ is the key for the ideal and modified AL preconditioners. This paper is meant to use the available Schur approximations for the original system (2), as introduced in Section 2, to construct a new approximation of S_γ. The new Schur complement approximation is realized by using the following lemma.

Lemma 3.1 *Assuming that all the relevant matrices are invertible, then the inverse of S_γ is given by*

$$S_\gamma^{-1} = S^{-1}(I - \gamma \widehat{C} W^{-1}) - \gamma W^{-1}, \tag{15}$$

where $S = -(\widehat{C} + B A^{-1} B^T)$ denotes the Schur complement of the original system (2) and $\widehat{C}$ is defined as $\widehat{C} = \nu^{-1} C$.

Proof. For the proof we refer to [4, 17]. ∎

Lemma 3.1 is originally revealed by [4] and used to derive the old approximation of S_γ, which is discussed in the next section. Here, Lemma 3.1 is viewed from another side. Since Lemma 3.1 builds the connection between the Schur complements S_γ and S, the natural and simple method to approximate S_γ is substituting the approximation of S into expression (15). In this way, the new approximation of S_γ, denoted by $\widetilde{S}_{\gamma\ \text{new}}$, is derived in the inverse form as

$$\widetilde{S}_{\gamma\ \text{new}}^{-1} = \widetilde{S}^{-1}(I - \gamma\widehat{C}W^{-1}) - \gamma W^{-1}, \tag{16}$$

where $\widetilde{S}$ denotes the approximation of S.

The novel approach provides a framework to use the known Schur complement approximation $\widetilde{S}$ for the original system (2) to construct $\widetilde{S}_{\gamma\ \text{new}}$ in the AL preconditioner, which is applied to the transformed system (13). Substituting the Schur complement approximations demonstrated in Section 2, i.e. $\widetilde{S}_{PCD}$, $\widetilde{S}_{LSC}$ and $\widetilde{S}_{SIMPLE}$ into expression (16), three variants of $\widetilde{S}_{\gamma\ \text{new}}$ are derived as

- $\widetilde{S}_{\gamma\ PCD}^{-1} = \widetilde{S}_{PCD}^{-1}(I - \gamma\widehat{C}W^{-1}) - \gamma W^{-1}$ with $\widetilde{S}_{PCD}$ defined by (9),
- $\widetilde{S}_{\gamma\ LSC}^{-1} = \widetilde{S}_{LSC}^{-1}(I - \gamma\widehat{C}W^{-1}) - \gamma W^{-1}$ with $\widetilde{S}_{LSC}$ defined by (10),
- $\widetilde{S}_{\gamma\ SIMPLE}^{-1} = \widetilde{S}_{SIMPLE}^{-1}(I - \gamma\widehat{C}W^{-1}) - \gamma W^{-1}$ with $\widetilde{S}_{SIMPLE}$ defined by (12).

Following other related references [3, 4], in this paper we choose the matrix parameter W to the diagonal approximation of the pressure mass matrix, i.e. $W = \widehat{M}_p = \text{diag}(M_p)$. It is trivial to obtain the action of W^{-1} in the transformation (13) and the new Schur complement approximation (16). Applying the new Schur complement approximation $\widetilde{S}_{\gamma\ \text{new}}$ converts to solve a system with it and the choice of $W = \widehat{M}_p$ focuses the complexity mainly on the solve of $\widetilde{S}$. This implies a limited increase of the complexity when implementing the new Schur complement approximation $\widetilde{S}_{\gamma\ \text{new}}$ compared to $\widetilde{S}$. In addition, the considerable efforts to optimize the approximation $\widetilde{S}$ can straightforwardly reduce the computational time of $\widetilde{S}_{\gamma\ \text{new}}$.

When applying stabilized FVM, the inverse of S_γ is expressed in a similar manner as Lemma 3.1 [18] and this similarity facilitates the extension of the new Schur complement approximation from the stabilized FVM to the stabilized FEM. Regarding the new Schur complement approximation, there are two main differences between [18] and this work. First, only $\widetilde{S}_{\gamma\ SIMPLE}$ is considered in [18] and in this paper we introduce three variants, i.e. $\widetilde{S}_{\gamma\ PCD}$, $\widetilde{S}_{\gamma\ LSC}$ and $\widetilde{S}_{\gamma\ SIMPLE}$. In this way, the comparison between them is expected to answer the questions raised in the introduction section. Second, In [18] finite volume discretization stabilized by the pressure-weighted interpolation method [26] is applied, which leads to $\widetilde{S}_{SIMPLE}$ in a reduced form. The generality is degraded since this special form of $\widetilde{S}_{SIMPLE}$ can not be obtained by using other stabilization and discretization methods in general. In this paper, the approximations $\widetilde{S}_{PCD}$, $\widetilde{S}_{LSC}$ and $\widetilde{S}_{SIMPLE}$ are expressed

in their defined manners so that a convincing assessment of the new Schur complement approximation can be expected.

Based on the above approach, it is easy to see that there is no extra requirement on the value of the parameter γ. This advantage of the new Schur complement approximation can be more clearly seen in the next section, where the contradictory requirements on the values of γ in the old approach are presented.

3.2 Old Schur approximation in the AL preconditioner

The starting point to construct the old approximation of the Schur complement in the AL preconditioner is also Lemma 3.1. However, the strategy is totally different. Choosing $W_1 = \gamma\widehat{C} + M_p$ and substituting W_1 into expression (15) we have

$$\begin{aligned} S_\gamma^{-1} &= S^{-1}(I - (\gamma\widehat{C} + M_p - M_p)(\gamma\widehat{C} + M_p)^{-1}) - \gamma(\gamma\widehat{C} + M_p)^{-1} \\ &= S^{-1}M_p(\gamma\widehat{C} + M_p)^{-1} - \gamma(\gamma\widehat{C} + M_p)^{-1} \\ &= (\gamma^{-1}S^{-1}M_p - I)(\widehat{C} + \gamma^{-1}M_p)^{-1}. \end{aligned}$$

For large values of γ such that $\| \gamma^{-1}S^{-1}M_p \| \ll 1$, the term $\gamma^{-1}S^{-1}M_p$ can be neglected so that we have $\widetilde{S}_{\gamma \text{ old}}$ as follows

$$\widetilde{S}_{\gamma \text{ old}} = -(\widehat{C} + \gamma^{-1}M_p). \tag{17}$$

The choice of $W_1 = \gamma\widehat{C} + M_p$ is not practical since the action of W_1^{-1} is needed in the transformed system (13). One practical choice is to omit the term γC in W_1 and replace M_p by its diagonal approximation, which leads to $W = \widehat{M_p}$. The choice of $W = \widehat{M_p}$ and $\widetilde{S}_{\gamma \text{ old}}$ is used in the related work, for instance [4, 17] where stabilized discretizations are employed.

The contradictory requirements in the above approximation are shown as follows. The approximation $\widetilde{S}_{\gamma \text{ old}}$ is obtained if and only if $W_1 = \gamma\widehat{C} + M_p$ and large values of γ are chosen. However, $W = \widehat{M_p}$ is spectrally equivalent to $W_1 = \gamma\widehat{C} + M_p$ only when γ is small. This means that it is contradictory to tune the value of γ so that $W = \widehat{M_p}$ and $\widetilde{S}_{\gamma \text{ old}}$ could be simultaneously obtained. By contrast, this contradictory requirements are avoided by applying the new Schur complement approximation as given in Section 3.1. This disadvantage of the old Schur complement approximation reflects in the slower convergence rate of the Krylov subspace solvers compared to the new Schur complement approximation. See more results in the numerical section.

3.3 Summary of the Schur complement approximations

At each Picard iteration, we solve either the transformed system (13) with the coefficient matrix $\mathcal{A}_\gamma$ or the original system (2) with the coefficient matrix $\mathcal{A}$. We apply the modified AL preconditioner $\mathcal{P}_{MAL}$ (14) and the block upper-triangular preconditioner $\mathcal{P}_U$ (8) to the

transformed and original systems, respectively. The Schur complement approximations applied in $\mathcal{P}_{MAL}$ and $\mathcal{P}_U$ are summarized in Table 1.

Table 1: Summary of the linear systems to be solved, applied preconditioners and approximations of the Schur complement utilized therein.

linear system	preconditioner	Schur complement approximations
transformed system with $\mathcal{A}_\gamma$	$\mathcal{P}_{MAL}$	$\widetilde{S}_{\gamma\ PCD}$, $\widetilde{S}_{\gamma\ LSC}$, $\widetilde{S}_{\gamma\ SIMPLE}$, $\widetilde{S}_{\gamma\ \text{old}}$
original system with $\mathcal{A}$	$\mathcal{P}_U$	$\widetilde{S}_{PCD}$, $\widetilde{S}_{LSC}$, $\widetilde{S}_{SIMPLE}$

With the choice of $W = \widehat{M}_p = \text{diag}(M_p)$ and definition of $\widehat{C} = \nu^{-1}C$, the Schur complement approximations applied in the modified AL preconditioner $\mathcal{P}_{MAL}$ are summarized as

1. $\widetilde{S}_{\gamma\ PCD}^{-1} = \widetilde{S}_{PCD}^{-1}(I - \gamma\widehat{C}\widehat{M}_p^{-1}) - \gamma\widehat{M}_p^{-1}$ with $\widetilde{S}_{PCD}$ as (9),
2. $\widetilde{S}_{\gamma\ LSC}^{-1} = \widetilde{S}_{LSC}^{-1}(I - \gamma\widehat{C}\widehat{M}_p^{-1}) - \gamma\widehat{M}_p^{-1}$ with $\widetilde{S}_{LSC}$ as (10),
3. $\widetilde{S}_{\gamma\ SIMPLE}^{-1} = \widetilde{S}_{SIMPLE}^{-1}(I - \gamma\widehat{C}\widehat{M}_p^{-1}) - \gamma\widehat{M}_p^{-1}$ with $\widetilde{S}_{SIMPLE}$ as (12),
4. $\widetilde{S}_{\gamma\ \text{old}} = -(\widehat{C} + \gamma^{-1}M_p)$.

The first three approximations are derived from the new approach $\widetilde{S}_{\gamma\ \text{new}}$ (16) and the last one corresponds to the old approach $\widetilde{S}_{\gamma\ \text{old}}$ (17).

As illustrated above, the new approximations of the Schur complement in the AL preconditioner involve the Schur complement approximations in the block upper-triangular preconditioner $\mathcal{P}_U$ for the original system. The Schur complement approximations used in $\mathcal{P}_U$ are given as follows

1. $\widetilde{S}_{PCD} = -L_p A_p^{-1} M_p$,
2. $\widetilde{S}_{LSC} = -(B\widehat{M}_u^{-1}B^T + C_1)(B\widehat{M}_u^{-1}A\widehat{M}_u^{-1}B^T + C_2)^{-1}(B\widehat{M}_u^{-1}B^T + C_1)$,
3. $\widetilde{S}_{SIMPLE} = -(\widehat{C} + B\text{diag}(A)^{-1}B^T)$.

Due to the small size of test problems and the lack of code optimization, the complexity comparison of preconditioners $\mathcal{P}_{MAL}$ and $\mathcal{P}_U$ is done based on the following costs analysis in this paper, instead of reporting the computational time. Firstly, we consider the costs of using the modified AL preconditioner $\mathcal{P}_{MAL}$ for a Krylov subspace method that solves the system with $\mathcal{A}_\gamma$. The preconditioner is applied at each Krylov iteration and the modified AL preconditioner involves the solution of the momentum sub-system 'mom-u' with $\widetilde{A}_\gamma$ and the pressure sub-system 'mass-p' with $\widetilde{S}_\gamma$. Furthermore, at each Krylov iteration additional costs are expressed in the product of the coefficient matrix $\mathcal{A}_\gamma$ with a Krylov residual vector $\mathbf{b_{res}}$. Thus, the total costs at each Krylov iteration are

- $\mathcal{P}_{MAL}$: mom-u with $\widetilde{A}_\gamma$ + mass-p with $\widetilde{S}_\gamma$ + $\mathcal{A}_\gamma \times \mathbf{b_{res}}$.

Clearly, the difference of costs by applying $\mathcal{P}_{MAL}$ arises from solving the pressure sub-system 'mass-p' with different Schur complement approximations. If we ignore the multiplications in the definition of the new Schur complement approximation $\widetilde{S}_{\gamma\ \text{new}}$, finding the solution of the pressure sub-system in $\mathcal{P}_{MAL}$ with three variants derived from $\widetilde{S}_{\gamma\ \text{new}}$, i.e., $\widetilde{S}_{\gamma\ PCD}$, $\widetilde{S}_{\gamma\ LSC}$ and $\widetilde{S}_{\gamma\ SIMPLE}$ is reduced to solve the pressure sub-system in $\mathcal{P}_U$ with $\widetilde{S}_{PCD}$, $\widetilde{S}_{LSC}$ and $\widetilde{S}_{SIMPLE}$, respectively. Systems involved in $\widetilde{S}_{PCD}$, $\widetilde{S}_{LSC}$ and $\widetilde{S}_{SIMPLE}$ are shown in Table 2. The costs of applying the old Schur complement approximation $\widetilde{S}_{\gamma\ \text{old}}$ are also included in Table 2 for a comparison with the new Schur complement approximation $\widetilde{S}_{\gamma\ \text{new}}$. Note that all involved systems are of the same size. If we assume a comparable complexity to solve different involved systems, the analysis in Table 2 shows that the costs of using $\mathcal{P}_{MAL}$ with $\widetilde{S}_{\gamma\ PCD}$ and $\widetilde{S}_{\gamma\ LSC}$ are roughly the same and two times of that with $\widetilde{S}_{\gamma\ SIMPLE}$ and $\widetilde{S}_{\gamma\ \text{old}}$.

Table 2: Pressure sub-system 'mass-p' with $\widetilde{S}_\gamma$ in $\mathcal{P}_{MAL}$ and $\widetilde{S}$ in $\mathcal{P}_U$, and the systems involved therein.

'mass-p' with $\widetilde{S}_{\gamma\ \text{new}}$	'mass-p' with $\widetilde{S}$	systems involved in $\widetilde{S}$
$\widetilde{S}_{\gamma\ PCD}$	$\widetilde{S}_{PCD}$	L_p and M_p
$\widetilde{S}_{\gamma\ LSC}$	$\widetilde{S}_{LSC}$	$(B\widehat{M}_u^{-1}B^T + C_1)$ twice
$\widetilde{S}_{\gamma\ SIMPLE}$	$\widetilde{S}_{SIMPLE}$	$\widehat{C} + B\text{diag}(A)^{-1}B^T$
'mass-p' with $\widetilde{S}_{\gamma\ \text{old}}$	–	systems involved in $\widetilde{S}_{\gamma\ \text{old}}$
$\widetilde{S}_{\gamma\ \text{old}}$	–	$\widehat{C} + \gamma^{-1}M_p$

Secondly, we consider the costs of applying the upper block-triangular preconditioner $\mathcal{P}_U$ with different Schur complement approximations, which are used for the original system. Similar to the analysis of $\mathcal{P}_{MAL}$, we obtain the total costs at every Krylov iteration as

- $\mathcal{P}_U$: mom-u with A + mass-p with $\widetilde{S}$ + $\mathcal{A} \times \mathbf{b_{res}}$.

Also, varying Schur complement approximations $\widetilde{S}$ results in the difference of costs by applying $\mathcal{P}_U$. Based on the analysis in Table 2 and the assumption of a comparable solution complexity for all involved systems, we find out that the costs of applying $\mathcal{P}_U$ with $\widetilde{S}_{PCD}$ and $\widetilde{S}_{LSC}$ are roughly the same and two times of that with $\widetilde{S}_{SIMPLE}$.

Lastly, we compare the costs between $\mathcal{P}_{MAL}$ and $\mathcal{P}_U$. As mentioned before, solving the pressure sub-system with the new Schur complement approximation $\widetilde{S}_{\gamma\ \text{new}}$ in $\mathcal{P}_{MAL}$ can be reduced to calculate the solution of the pressure sub-system with $\widetilde{S}$, which is the Schur complement approximation used in $\mathcal{P}_U$. Thus, the difference of costs between $\mathcal{P}_{MAL}$ and $\mathcal{P}_U$ focuses on the solution of the momentum sub-system and the product of the coefficient matrix with the Krylov residual vector. More non-zero fill-in in A_γ and $\mathcal{A}_\gamma$ [17], compared

to A and $\mathcal{A}$, results in a heavier matrix-vector product when applying $\mathcal{P}_{MAL}$ at each Krylov iteration. However, the heavier complexity of $\mathcal{P}_{MAL}$ could be paid off by a reduced number of Krylov iterations. In this paper we obtain a faster convergence rate preconditioned by $\mathcal{P}_{MAL}$ with the new Schur complement approximations, compared to $\mathcal{P}_U$ used for the original system. The time advantage of $\mathcal{P}_{MAL}$ needs a further assessment which is included in future research plan.

4 Numerical experiments

In this section, we carry out numerical experiments on the following 2D laminar benchmarks:

(1) **Flow over a finite flat plate (FP)**
This example, known as Blasius flow, models a boundary layer flow over a flat plate on the domain $\Omega = (-1, 5) \times (-1, 1)$. To model this flow, the Dirichlet boundary condition $u_x = 1, u_y = 0$ is imposed at the inflow boundary ($x = -1$; $-1 \leq y \leq 1$) and also on the top and bottom of the channel ($-1 \leq x \leq 5$; $y = \pm 1$), representing walls moving from left to right with speed unity. The plate is modeled by imposing a no-flow condition on the internal boundary ($0 \leq x \leq 5$; $y = 0$), and the Neumann condition is applied at the outflow boundary ($x = 5$; $-1 < y < 1$), i.e., $\nu \frac{\partial \mathbf{u}}{\partial \mathbf{n}} - \mathbf{n}p = \mathbf{0}$. The Reynolds number is defined by $Re = UL/\nu$ and the reference velocity and length are chosen as $U = 1$ and $L = 5$. On the FP flow, we consider four Reynolds numbers as $Re = \{10^2, 10^3, 10^4, 10^5\}$, which correspond to the viscosity parameters $\nu = \{5 \cdot 10^{-2}, 5 \cdot 10^{-3}, 5 \cdot 10^{-4}, 5 \cdot 10^{-5}\}$, respectively.

Since stretched grid is typically needed to compute the flow accurately at large Reynolds numbers, stretched grid is generated based on the uniform Cartesian grid with $12 \times 2^n \cdot 2^n$ cells. The stretching function is applied in the y-direction with the parameter $b = 1.01$ [c.f. [24]]:

$$y = \frac{(b+1) - (b-1)c}{(c+1)}, \quad c = (\frac{b+1}{b-1})^{1-\bar{y}}, \quad \bar{y} = 0, 1/n, 2/n, ...1. \tag{18}$$

(2) **Flow over backward facing step (BFS)**
The L-shaped domain is known as the backward facing step. A Poisseuille flow profile is imposed on the inflow ($x = -1; 0 \leq y \leq 1$). No-slip boundary conditions are imposed on the walls. The Neumann condition is applied at the outflow ($x = 5; -1 < y < 1$) which automatically sets the outflow pressure to zero. Using the reference velocity and length $U = 1$ and $L = 2$ and the viscosity parameters $\nu = \{2 \cdot 10^{-2}, 2 \cdot 10^{-3}\}$, the corresponding Reynolds numbers are $Re = UL/\nu = \{10^2, 10^3\}$.

The BFS flow is more complicated than the flat-plate flow as it features separation, a free shear-layer and reattachment. On the BFS flow we do not consider the Reynolds number $Re > 10^3$ since the increase of the Reynolds number by an order of magnitude

will transfer the flow to be turbulent. On this case we only consider uniform Cartesian grid with $11 \times 2^n \cdot 2^n$ cells.

(3) **Lid driven cavity (LDC)**
This problem simulates the flow in a square cavity $(-1, 1)^2$ with enclosed boundary conditions. A lid moving from left to right with a horizontal velocity as:

$$u_x = 1 - x^4 \quad \text{for} \quad -1 \leq x \leq 1 \quad y = 1.$$

In order to accurately resolve the small recirculations, we consider stretched grid around the four corners. Stretched grid is generated based on the uniform Cartesian grid with $2^n \cdot 2^n$ cells. The stretching function is applied in both directions with parameters $a = 0.5$ and $b = 1.01$ [24]

$$x = \frac{(b + 2a)c - b + 2a}{(2a + 1)(1 + c)}, c = (\frac{b + 1}{b - 1})^{\frac{\bar{x}-a}{1-a}}, \bar{x} = 0, 1/n, 2/n, ..., 1. \tag{19}$$

The reference velocity and length $U = 1$ and $L = 2$ and the viscosity parameters $\nu = \{2 \cdot 10^{-2}, 2 \cdot 10^{-3}, 2 \cdot 10^{-4}\}$ result in the following Reynolds numbers $Re = \{10^2, 10^3, 10^4\}$. For the same reason as BFS, a larger Reynolds number $Re > 10^4$ is not considered on this case.

In order to explore the performance of $\mathcal{P}_{MAL}$ and $\mathcal{P}_U$ with varying Schur complement approximations as summarized in Table 1 and Table 2, numerical evaluations are classified into four categories as follows.

(C1) **On small Reynolds number and uniform grid**
In this category we consider the FP, BFS and LDC cases on the small Reynolds number $Re = 10^2$ and uniform Cartesian grid.

(C2) **On moderate Reynolds number and uniform grid**
In this category we apply the moderate Reynolds number $Re = 10^3$ on the FP, BFS and LDC cases. Similar to the first class of experiments, uniform Cartesian grid is used here to check the variation of performance when increasing the Reynolds number by an order of magnitude.

(C3) **On moderate Reynolds numbers and stretched grid**
This category contains the tests carried out on the FP and LDC cases with stretched grid. The stretching functions for the FP and LDC cases are (18) and (19), respectively. Still, the moderate Reynolds number $Re = 10^3$ is employed for the two tests. Comparing with the second class of experiments, this category is meant to investigate the effect of mesh anisotropy.

(C4) **On large Reynolds numbers and stretched grid**
The LDC case with $Re = 10^4$ and FP case with $Re = \{10^4, 10^5\}$ are included in this class of tests to assess how the Krylov subspace solver behaves at relatively large Reynolds numbers. Here stretched grid is employed to accurately resolve the problem characteristics.

In this paper all experiments are carried out based on the blocks A, B, C, C_1, C_2, A_p, M_p, L_p and M_u and the right-hand side vector rhs, which are obtained at the middle step of the whole nonlinear iterations. Numerical experiments in [17] show that the number of linear iterations varies during the nonlinear procedure. The motivation of choosing the middle step of the nonlinear iterations to export the blocks and vector is that a representative number of linear iteration can be obtained, compared to the averaged number of linear iterations through the whole nonlinear procedure. The relative stopping tolerance to solve the linear system by GMRES is chosen equal to 10^{-8}. The restart functionality of GMRES is not used in this paper. Since the preconditioners $\mathcal{P}_{MAL}$ and $\mathcal{P}_U$ involve various momentum and pressure sub-systems, all these sub-systems are directly solved in this paper to avoid the sensitiveness of iterative solvers on the varying solution complexities.

As pointed out in Section 2, the application of the Schur complement approximation $\widetilde{S}_{\gamma\ PCD}$ needs to preset boundary conditions for the pressure Laplacian L_p and convection-diffusion A_p operators. In this paper, we follow the suggestions of [10, 19] to use Dirichlet boundary conditions along inflow boundaries to define L_p and A_p. This means that the rows and columns of L_p and A_p corresponding to the pressure nodes on an inflow boundary are treated as though they are associated with Dirichlet boundary conditions. For the enclosed flow, we algebraically add $h^2 I$ to L_p and A_p to make them non-singular, where h denotes the grid size and I is the identity matrix of proper size. Such artificial pressure boundary conditions are only imposed on the preconditioner. The coefficient matrix and right-hand side vector are not affected by these boundary node modifications.

4.1 On small Reynolds number and uniform grid

In this subsection we carry out experiments on the FP, BFS and LDC cases with uniform Cartesian grid and small Reynolds number $Re = 10^2$. The number of Krylov iterations to solve the transformed system preconditioned by the modified AL preconditioner $\mathcal{P}_{MAL}$ is given in Table 3. The Schur complement approximations $\widetilde{S}_{\gamma\ PCD}$, $\widetilde{S}_{\gamma\ LSC}$, $\widetilde{S}_{\gamma\ SIMPLE}$ in $\mathcal{P}_{MAL}$ are derived from the new method $\widetilde{S}_{\gamma\ \text{new}}$ (16) and the approximation $\widetilde{S}_{\gamma\ \text{old}}$ corresponds to the old Schur complement approximation (17). In this paper, the reported number of Krylov iterations is obtained by using the optimal value of γ, which results in the fastest convergence rate of the Krylov subspace solver. The following observations are made from Table 3.

Except $\widetilde{S}_{\gamma\ SIMPLE}$, we see that the other Schur complement approximations result in the independence of Krylov iterations on the mesh refinement at the three test cases. In terms of the number of Krylov iterations, $\widetilde{S}_{\gamma\ LSC}$ is superior to the other Schur complement approximations on the FP and BFS cases by the reduced number of iterations and equally efficient as $\widetilde{S}_{\gamma\ PCD}$ and $\widetilde{S}_{\gamma\ \text{old}}$ on the LDC case. To understand this advantage, we take the FP case as an example and plot the eigenvalues of the preconditioned Schur complement matrix $\widetilde{S}_\gamma^{-1} S_\gamma$ in Figure 1. As can be seen, $\widetilde{S}_{\gamma\ LSC}$ leads to more clustered eigenvalues and the smallest eigenvalue further away from zero. Such a distribution of eigenvalues is favorable for the Krylov subspace solver and a faster convergence rate can be expected. We know that there can be matrices where there is no relation between the spectrum and the

convergence of GMRES [14], especially if the matrix is strongly non normal. We include the spectrum because in our examples the properties of the spectrum are in line with the convergence properties of GMRES.

As analyzed in Section 3.3, at each Krylov iteration the costs of applying $\mathcal{P}_{MAL}$ with $\widetilde{S}_{\gamma\ LSC}$ are roughly the same as $\widetilde{S}_{\gamma\ PCD}$ and two times of that using $\widetilde{S}_{\gamma\ SIMPLE}$ and $\widetilde{S}_{\gamma\ \text{old}}$. If we assume the computational expense of applying $\mathcal{P}_{MAL}$ with $\widetilde{S}_{\gamma\ \text{old}}$ to be unit at each iteration, the total costs by using all Schur complement approximations on the finest grid are presented in Table 4 and calculated by multiplying the expense per iteration by the number of iterations. In the other classes of evaluations we also use this method to calculate the total computational costs.

Results in Table 4 show that the minimal computational costs are achieved by using $\widetilde{S}_{\gamma\ \text{old}}$ in $\mathcal{P}_{MAL}$. Although less Krylov iterations are needed by using $\widetilde{S}_{\gamma\ LSC}$ in $\mathcal{P}_{MAL}$ seen from Table 3, the reduced number of iterations does not pay off the heavier costs of $\widetilde{S}_{\gamma\ LSC}$. In this class of experiments, it seems that the old Schur complement approximation $\widetilde{S}_{\gamma\ \text{old}}$ is more efficient than the other approximations due to the less computational costs in total.

Table 3: $\mathbf{Re = 10^2}$ and **uniform grid**: the number of GMRES iterations to solve the transformed system with $\mathcal{A}_\gamma$ preconditioned by $\mathcal{P}_{MAL}$ with different Schur complement approximations and the optimal value of γ in parentheses.

	$\widetilde{S}_{\gamma\ PCD}$	$\widetilde{S}_{\gamma\ LSC}$	$\widetilde{S}_{\gamma\ SIMPLE}$	$\widetilde{S}_{\gamma\ \text{old}}$
FP case:				
$n = 5$	26(1.e-1)	17(8.e-2)	43(2.e-1)	38(2.e-1)
$n = 6$	25(1.e-1)	25(8.e-2)	67(2.e-1)	38(2.e-1)
$n = 7$	25(1.e-1)	26(8.e-2)	100(2.e-1)	38(2.e-1)
BFS case:				
$n = 5$	34(2.e-2)	17(2.e-2)	42(1.e-1)	36(1.e-1)
$n = 6$	42(3.e-2)	21(2.e-2)	60(1.e-1)	36(1.e-1)
$n = 7$	45(3.e-2)	22(2.e-2)	87(1.e-1)	36(1.e-1)
LDC case:				
$n = 6$	17(2.e-2)	17(2.e-2)	34(1.e-1)	19(1.e-1)
$n = 7$	18(2.e-2)	20(2.e-2)	48(1.e-1)	19(1.e-1)
$n = 8$	18(2.e-2)	22(2.e-2)	63(1.e-1)	19(1.e-1)

Table 4: $\mathbf{Re = 10^2}$ and **uniform grid**: the total costs of applying $\mathcal{P}_{MAL}$ with different Schur complement approximations on the finest uniform Cartesian grid.

	$\widetilde{S}_{\gamma\ PCD}$	$\widetilde{S}_{\gamma\ LSC}$	$\widetilde{S}_{\gamma\ SIMPLE}$	$\widetilde{S}_{\gamma\ \text{old}}$
FP case:	50	52	100	38
BFS case:	90	44	87	36
LDC case:	36	44	63	19

Figure 1: **FP** and $\mathbf{Re = 10^2}$: plot of eigenvalues of the preconditioned matrices $\widetilde{S}_\gamma^{-1}S_\gamma$ at the uniform Cartesian grid with $12 \times 2^5 \cdot 2^5$ cells.

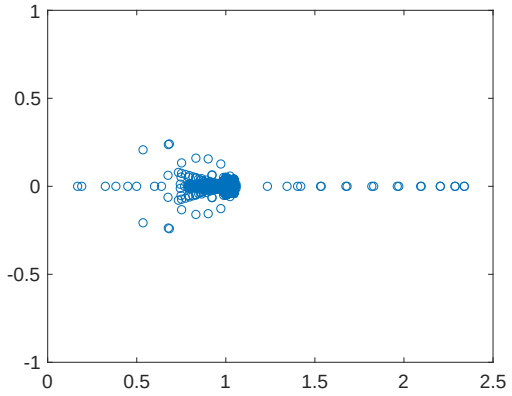

(a) $\widetilde{S}_{\gamma\ PCD}^{-1}S_\gamma$, $\gamma = 0.1$

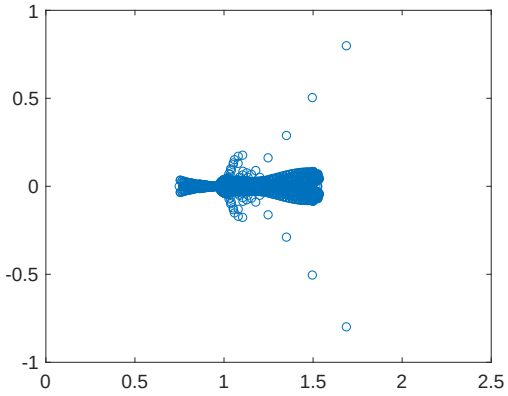

(b) $\widetilde{S}_{\gamma\ LSC}^{-1}S_\gamma$, $\gamma = 0.08$

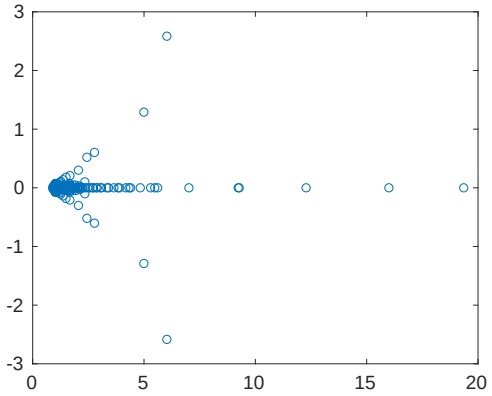

(c) $\widetilde{S}_{\gamma\ SIMPLE}^{-1}S_\gamma$, $\gamma = 0.2$

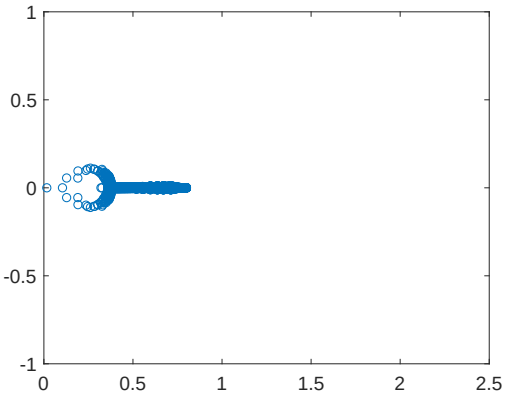

(d) $\widetilde{S}_{\gamma\ \text{old}}^{-1}S_\gamma$, $\gamma = 0.2$

4.2 On moderate Reynolds number and uniform grid

In this subsection we choose the moderate Reynolds number $Re = 10^3$ to evaluate the performance of the Schur complement approximations used in the modified AL preconditioner

$\mathcal{P}_{MAL}$ and compare with the evaluations at $Re = 10^2$ in Section 4.1. Based on the number of Krylov iterations presented in Table 5, we see that the independence of Krylov iterations on the mesh refinement is achieved by using the Schur complement approximations $\widetilde{S}_{\gamma\ PCD}$ and $\widetilde{S}_{\gamma\ LSC}$ in $\mathcal{P}_{MAL}$, which is also observed in Section 4.1. Contrary to the observations in Section 4.1, the old Schur complement approximation $\widetilde{S}_{\gamma\ \text{old}}$ does not result in the mesh independence of Krylov iterations at $Re = 10^3$. With the utilization of $\widetilde{S}_{\gamma\ SIMPLE}$ the number of Krylov iterations is dependent of the grid size at both $Re = 10^2$ and 10^3.

Results in Table 5 show that the smallest number of Krylov iterations is obtained by using $\widetilde{S}_{\gamma\ LSC}$ in $\mathcal{P}_{MAL}$, which also results in the minimal total costs in Table 6. The total costs are calculated by using the same method as Section 4.2. Taking the mesh independence into account, the utilization of $\widetilde{S}_{\gamma\ LSC}$ will lead to a further reduction of total costs on finer grids over $\widetilde{S}_{\gamma\ SIMPLE}$ and $\widetilde{S}_{\gamma\ \text{old}}$, which require more iterations with mesh refinement. Compared to $\widetilde{S}_{\gamma\ PCD}$ which also results in the mesh independence of Krylov iterations, the application of $\widetilde{S}_{\gamma\ LSC}$ reduces the total computational costs at least two times on the FP and BFS cases, and this reduction factor can also be expected on finer grids. On the LDC case $\widetilde{S}_{\gamma\ LSC}$ is equally efficient as $\widetilde{S}_{\gamma\ PCD}$.

For the tests at $Re = 10^3$ it shows that $\widetilde{S}_{\gamma\ LSC}$ is superior to the other Schur complement approximations by the reduction of Krylov iterations and total computational costs. In the first class of tests with $Re = 10^2$, the superiority of $\widetilde{S}_{\gamma\ \text{old}}$ is seen. This implies that the optimal Schur complement approximation in $\mathcal{P}_{MAL}$ depends on the Reynolds number.

Table 5: $\mathbf{Re = 10^3}$ and **uniform grid**: the number of GMRES iterations to solve the transformed system with $\mathcal{A}_\gamma$ preconditioned by $\mathcal{P}_{MAL}$ with different Schur complement approximations and the optimal value of γ in parentheses.

	$\widetilde{S}_{\gamma\ PCD}$	$\widetilde{S}_{\gamma\ LSC}$	$\widetilde{S}_{\gamma\ SIMPLE}$	$\widetilde{S}_{\gamma\ \text{old}}$
FP case:				
$n = 5$	54(8.e-3)	29(8.e-3)	34(2.e-2)	76(6.e-2)
$n = 6$	55(8.e-3)	18(8.e-3)	51(2.e-2)	90(6.e-2)
$n = 7$	56(8.e-3)	17(8.e-3)	99(2.e-2)	95(6.e-2)
BFS case:				
$n = 5$	66(4.e-3)	45(3.e-3)	49(1.e-2)	71(3.e-2)
$n = 6$	63(4.e-3)	27(3.e-3)	77(1.e-2)	76(3.e-2)
$n = 7$	65(3.e-3)	29(3.e-3)	142(1.e-2)	84(3.e-2)
LDC case:				
$n = 6$	30(4.e-3)	54(1.e-3)	66(7.e-3)	36(2.e-2)
$n = 7$	28(4.e-3)	29(4.e-3)	52(1.e-2)	42(2.e-2)
$n = 8$	29(4.e-3)	29(4.e-3)	85(1.e-2)	48(2.e-2)

Table 6: $\mathbf{Re = 10^3}$ and **uniform grid**: the total costs of applying $\mathcal{P}_{MAL}$ with different Schur complement approximations on the finest uniform Cartesian grid.

	$\widetilde{S}_{\gamma\ PCD}$	$\widetilde{S}_{\gamma\ LSC}$	$\widetilde{S}_{\gamma\ SIMPLE}$	$\widetilde{S}_{\gamma\ \text{old}}$
FP case:	112	34	99	95
BFS case:	130	58	142	84
LDC case:	58	58	85	48

4.3 On moderate Reynolds number and stretched grid

Table 7: $\mathbf{Re = 10^3}$ and **stretched grid**: the number of GMRES iterations to solve the transformed system with $\mathcal{A}_\gamma$ preconditioned by $\mathcal{P}_{MAL}$ with different Schur complement approximations and the optimal value of γ in parentheses.

	$\widetilde{S}_{\gamma\ PCD}$	$\widetilde{S}_{\gamma\ LSC}$	$\widetilde{S}_{\gamma\ SIMPLE}$	$\widetilde{S}_{\gamma\ \text{old}}$
FP case:				
$n = 5$	59(8.e-3)	90(7.e-3)	37(2.e-2)	69(6.e-2)
$n = 6$	66(8.e-3)	89(7.e-3)	63(2.e-2)	85(6.e-2)
$n = 7$	62(8.e-3)	117(6.e-3)	119(2.e-2)	92(6.e-2)
LDC case:				
$n = 6$	65(2.e-3)	98(2.e-3)	57(7.e-3)	69(1.e-2)
$n = 7$	41(2.e-3)	58(2.e-3)	46(7.e-3)	40(1.e-2)
$n = 8$	38(2.e-3)	84(2.e-3)	75(7.e-3)	54(1.e-2)

Table 8: $\mathbf{Re = 10^3}$ and **stretched grid**: the total costs of applying $\mathcal{P}_{MAL}$ with different Schur complement approximations on the finest stretched grid.

	$\widetilde{S}_{\gamma\ PCD}$	$\widetilde{S}_{\gamma\ LSC}$	$\widetilde{S}_{\gamma\ SIMPLE}$	$\widetilde{S}_{\gamma\ \text{old}}$
FP case:	124	234	119	92
LDC case:	76	168	75	54

This subsection is meant to investigate the influence of mesh anisotropy on the performance of the modified AL preconditioner $\mathcal{P}_{MAL}$. To compare with Section 4.2, we apply the stretched grid and moderate Reynolds number $Re = 10^3$ on the FP and LDC cases. The number of Krylov iterations and total computational costs are presented in Table 7 and Table 8, respectively. From Table 7 we note that only $\widetilde{S}_{\gamma\ PCD}$ results in the mesh

independence and the minimal number of Krylov iterations. Although the total costs of applying $\widetilde{S}_{\gamma\ PCD}$ are more than that by using $\widetilde{S}_{\gamma\ SIMPLE}$ and $\widetilde{S}_{\gamma\ \text{old}}$ on the considered finest grid, as seen from Table 8, less costs in total by using $\widetilde{S}_{\gamma\ PCD}$ can be expected on finer grids due to the mesh independence. Therefore, we think that $\widetilde{S}_{\gamma\ PCD}$ is superior to the other Schur complement approximations on the tests with $Re = 10^3$ and stretched grid.

Note that on the FP and LDC cases with stretched grid, $\mathcal{P}_{MAL}$ with $\widetilde{S}_{\gamma\ LSC}$ is not mesh independent any more and performs the worst. This is contrary to the observations with uniform Cartesian grid seen in Section 4.2. To check the effect of mesh anisotropy, we put the number of Krylov iterations on both uniform and stretched grids together. In this way, Table 9 and Table 10 are generated for the FP and LDC cases respectively, and from them we clearly see that mesh anisotropy deteriorates the efficiency of $\widetilde{S}_{\gamma\ LSC}$. Considering the FP case as an example, on the finest stretched grid of $n = 7$ the number of Krylov iterations preconditioned by $\mathcal{P}_{MAL}$ with $\widetilde{S}_{\gamma\ LSC}$ increases by a factor about 7 compared to the finest uniform grid. The less efficiency of $\mathcal{P}_{MAL}$ with $\widetilde{S}_{\gamma\ LSC}$ arising from the mesh anisotropy is also seen on the LDC case from Table 10. On the other hand, the number of Krylov iterations preconditioned by $\mathcal{P}_{MAL}$ with the other Schur complement approximations seems robust with respect to mesh anisotropy on the FP and LDC cases.

The less efficiency of $\widetilde{S}_{\gamma\ LSC}$ on the stretched grid can be explained by the results in Figure 2, where we consider the FP case at $Re = 10^3$ and plot the eigenvalues of the preconditioned matrix $\widetilde{S}^{-1}_{\gamma\ LSC} S_\gamma$ for both uniform and stretched grids. As seen from Figure 2, stretching the grid considerably spreads the distribution of the eigenvalues of the preconditioned Schur complement $\widetilde{S}^{-1}_{\gamma\ LSC} S_\gamma$, which makes the convergence of the Krylov subspace solver more difficult.

Table 9: **FP** and $\mathbf{Re = 10^3}$: the number of GMRES iterations to solve the transformed system with $\mathcal{A}_\gamma$ preconditioned by $\mathcal{P}_{MAL}$ with different Schur complement approximations and the optimal value of γ in parentheses. Both the uniform and stretched grids are applied.

	$\widetilde{S}_{\gamma\ PCD}$	$\widetilde{S}_{\gamma\ LSC}$	$\widetilde{S}_{\gamma\ SIMPLE}$	$\widetilde{S}_{\gamma\ \text{old}}$
uniform grid				
$n = 5$	54(8.e-3)	29(8.e-3)	34(2.e-2)	76(6.e-2)
$n = 6$	55(8.e-3)	18(8.e-3)	51(2.e-2)	90(6.e-2)
$n = 7$	56(8.e-3)	17(8.e-3)	99(2.e-2)	95(6.e-2)
stretched grid				
$n = 5$	59(8.e-3)	90(7.e-3)	37(2.e-2)	69(6.e-2)
$n = 6$	66(8.e-3)	89(7.e-3)	63(2.e-2)	85(6.e-2)
$n = 7$	62(8.e-3)	117(6.e-3)	119(2.e-2)	92(6.e-2)

Table 10: **LDC** and $\mathbf{Re = 10^3}$: the number of GMRES iterations to solve the transformed system with $\mathcal{A}_\gamma$ preconditioned by $\mathcal{P}_{MAL}$ with different Schur complement approximations and the optimal value of γ in parentheses. Both the uniform and stretched grids are applied.

	$\widetilde{S}_{\gamma\ PCD}$	$\widetilde{S}_{\gamma\ LSC}$	$\widetilde{S}_{\gamma\ SIMPLE}$	$\widetilde{S}_{\gamma\ \text{old}}$
uniform grid				
$n = 6$	30(4.e-3)	54(1.e-3)	66(7.e-3)	36(2.e-2)
$n = 7$	28(4.e-3)	29(4.e-3)	52(1.e-2)	42(2.e-2)
$n = 8$	29(4.e-3)	29(4.e-3)	85(1.e-2)	48(2.e-2)
stretched grid				
$n = 6$	65(2.e-3)	98(2.e-3)	57(7.e-3)	69(1.e-2)
$n = 7$	41(2.e-3)	58(2.e-3)	46(7.e-3)	40(1.e-2)
$n = 8$	38(2.e-3)	84(2.e-3)	75(7.e-3)	54(1.e-2)

Figure 2: **FP** and $\mathbf{Re = 10^3}$: plot of eigenvalues of the preconditioned matrices $\widetilde{S}_{\gamma\ LSC}^{-1} S_\gamma$ at the uniform Cartesian and stretched grids with $12 \times 2^5 \cdot 2^5$ cells.

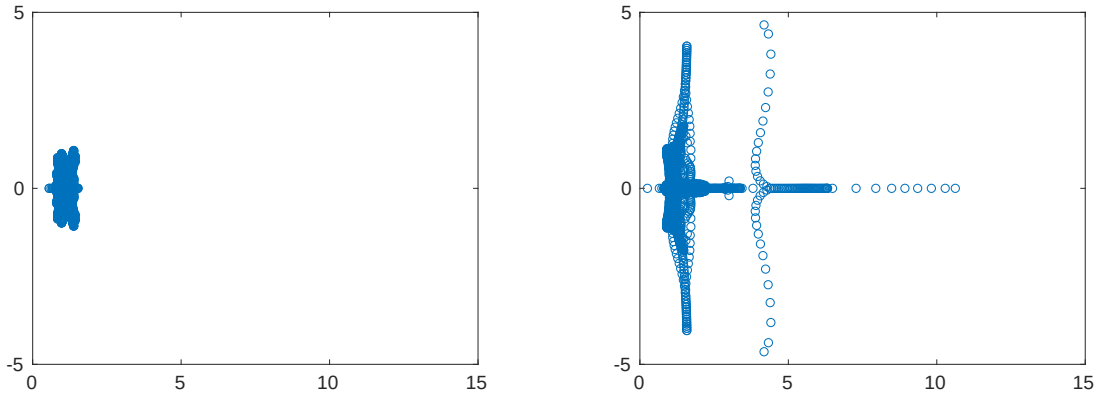

(a) uniform grid, $\gamma = 8.\text{e-}3$

(b) stretched grid, $\gamma = 7.\text{e-}3$

4.4 On large Reynolds number and stretched grid

In this subsection we apply large Reynolds numbers $Re \geq 10^4$ and stretched grids on the LDC and FP cases. Results in Table 11 and Table 12 illustrate that the fastest convergence rate of the Krylov subspace solver and the minimal computational costs in total are achieved by using $\widetilde{S}_{\gamma\ SIMPLE}$ in $\mathcal{P}_{MAL}$ on the two tests. Taking the FP case at $Re = 10^4$ as an example, from Table 12 we see that the utilization of $\widetilde{S}_{\gamma\ SIMPLE}$ reduces the total costs at least two times with respect to the other Schur approximations. The reduction factor turns to five at least when applying an even larger Reynolds number $Re = 10^5$ on

the FP case, which is seen from Table 13. In the context of large Reynolds numbers, it appears that $\widetilde{S}_{\gamma\ SIMPLE}$ is the optimal Schur complement approximation in the modified AL preconditioner $\mathcal{P}_{MAL}$. In contrast to the previous tests, at large Reynolds numbers none of the considered Schur complement approximations lead to the mesh independence of $\mathcal{P}_{MAL}$. The reason and possible improvement on this issue are to be explored in future research.

To investigate the effect of the Reynolds number, we take the FP case as an example and in Figure 3 plot the number of Krylov iterations preconditioned by $\mathcal{P}_{MAL}$ at varying Reynolds numbers. It appears that only $\widetilde{S}_{\gamma\ SIMPLE}$ results in the robustness of $\mathcal{P}_{MAL}$ with respect to the Reynolds number. To understand the reasons, we compute the extremal eigenvalues of the preconditioned Schur complement matrix $\widetilde{S}_{\gamma}^{-1}S_{\gamma}$ and present them in Table 14. R_{min} and R_{max} denote the smallest and largest real parts of the eigenvalues and I_{max} corresponds the largest imaginary part. These extremal values correspond to the boundaries of the rectangular domain containing all eigenvalues. Regarding $\widetilde{S}_{\gamma\ SIMPLE}^{-1}S_{\gamma}$, the values of R_{min} slightly decrease and remain the same order of magnitude. Together with the decrease of R_{max}/R_{min} and I_{max}, the eigenvalues are further clustered. However, less clustered eigenvalues are yielded by using the other Schur complement approximations. This explains the robustness of $\mathcal{P}_{MAL}$ with $\widetilde{S}_{\gamma\ SIMPLE}$ with respect to the Reynolds number.

Table 11: $\mathbf{Re = 10^4}$ and **stretched grid**: the number of GMRES iterations to solve the transformed system with $\mathcal{A}_{\gamma}$ preconditioned by $\mathcal{P}_{MAL}$ with different Schur complement approximations and the optimal value of γ in parentheses.

	$\widetilde{S}_{\gamma\ PCD}$	$\widetilde{S}_{\gamma\ LSC}$	$\widetilde{S}_{\gamma\ SIMPLE}$	$\widetilde{S}_{\gamma\ \text{old}}$
FP case:				
$n = 5$	363(8.e-4)	369(6.e-4)	35(2.e-3)	93(1.e-2)
$n = 6$	334(8.e-4)	336(6.e-4)	53(3.e-3)	128(2.e-2)
$n = 7$	346(8.e-4)	374(6.e-4)	83(4.e-3)	192(2.e-2)
LDC case:				
$n = 6$	113(3.e-4)	97(2.e-4)	34(1.e-3)	46(5.e-3)
$n = 7$	143(3.e-4)	235(2.e-4)	45(1.e-3)	65(5.e-3)
$n = 8$	159(4.e-4)	309(2.e-4)	80(2.e-3)	106(5.e-3)

Table 12: $\mathbf{Re = 10^4}$ and **stretched grid**: the total costs of applying $\mathcal{P}_{MAL}$ with different Schur complement approximations on the finest stretched grid.

	$\widetilde{S}_{\gamma\ PCD}$	$\widetilde{S}_{\gamma\ LSC}$	$\widetilde{S}_{\gamma\ SIMPLE}$	$\widetilde{S}_{\gamma\ \text{old}}$
FP case:	692	748	83	192
LDC case:	318	618	80	106

Table 13: **FP** and $\mathbf{Re = 10^5}$: the number of GMRES iterations and total costs to solve the transformed system with $\mathcal{A}_\gamma$ preconditioned by $\mathcal{P}_{MAL}$ with different Schur complement approximations and the optimal value of γ in parentheses. The stretched grid is applied.

	$\widetilde{S}_{\gamma\ PCD}$	$\widetilde{S}_{\gamma\ LSC}$	$\widetilde{S}_{\gamma\ SIMPLE}$	$\widetilde{S}_{\gamma\ \text{old}}$
iterations:				
$n = 5$	1000+	1000+	26(1.e-4)	136(1.e-3)
$n = 6$	1000+	1000+	35(2.e-4)	192(2.e-3)
$n = 7$	1000+	1000+	58(3.e-4)	310(2.e-3)
total costs:				
$n = 7$	2000+	2000+	58	310

Figure 3: **FP** and **stretched grid**: plot of the number of GMRES iterations preconditioned by $\mathcal{P}_{MAL}$ at varying Reynolds numbers.

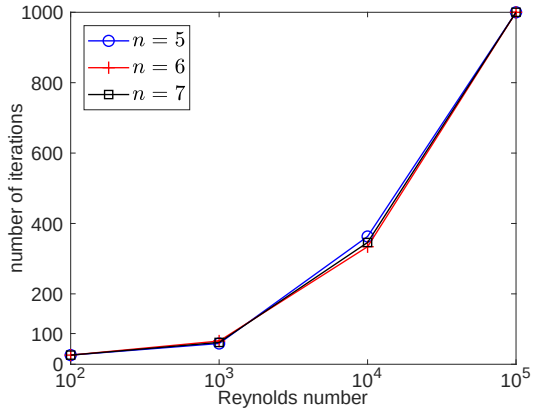

(a) $\mathcal{P}_{MAL}$ with $\widetilde{S}_{\gamma\ PCD}$

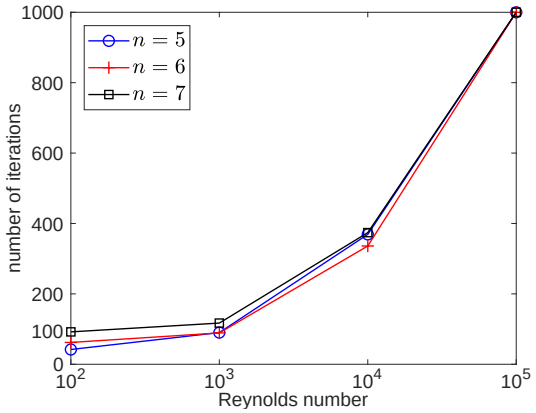

(b) $\mathcal{P}_{MAL}$ with $\widetilde{S}_{\gamma\ LSC}$

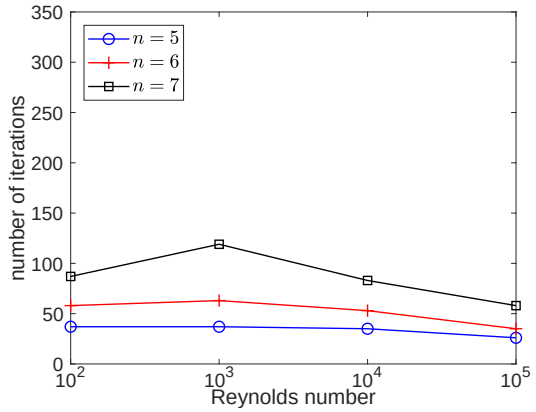

(c) $\mathcal{P}_{MAL}$ with $\widetilde{S}_{\gamma\ SIMPLE}$

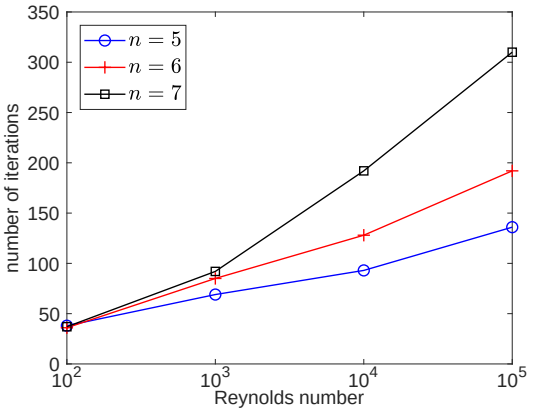

(d) $\mathcal{P}_{MAL}$ with $\widetilde{S}_{\gamma\ \text{old}}$

4.5 Summary of the Schur complement approximations in $\mathcal{P}_{MAL}$

Based on the above four classes of numerical evaluations, in Table 15 we summarize the optimal Schur complement approximation in the modified AL preconditioner $\mathcal{P}_{MAL}$. It shows that the optimal Schur complement approximation, which leads to the fastest convergence rate of the Krylov subspace solver, depends on the Reynolds number and mesh anisotropy. At every class of evaluations, the optimal Schur complement approximation is problem independent. Numerical evaluations in this paper show that $\widetilde{S}_{\gamma\ \text{old}}$ is suitable for the calculations with small Reynolds numbers and $\widetilde{S}_{\gamma\ SIMPLE}$ delivers a better performance for large Reynolds numbers due to its Reynolds robustness. In the context of moderate Reynolds numbers, $\widetilde{S}_{\gamma\ LSC}$ is more efficient with uniform grids but sensitive to mesh anisotropy. When stretched grids are employed, $\widetilde{S}_{\gamma\ PCD}$ turns out to be the optimal choice in the moderate Reynolds number context. Except the calculations at small Reynolds numbers and uniform grids, the optimal Schur complement approximations on

other classes of tests are derived from the new method $\widetilde{S}_{\gamma\ \mathrm{new}}$ proposed in this paper. This demonstrates the advantage of the new approach over the traditional one $\widetilde{S}_{\gamma\ \mathrm{old}}$. The mesh independence of Krylov iterations is not achieved by using the optimal Schur complement approximation only for the class of tests with large Reynolds numbers. The reason and possible improvement on this issue are to be considered in future research.

Table 14: **FP** and **stretched grid**: the extremal eigenvalues of the preconditioned Schur complement $\widetilde{S}_{\gamma}^{-1}S_{\gamma}$ at varying Reynolds numbers. The stretched grid with $12 \times 2^5 \cdot 2^5$ cells is used. R_{min} and R_{max} denote the smallest and largest real parts of the eigenvalues and I_{max} corresponds the largest imaginary part.

	$Re = 10^2$	$Re = 10^3$	$Re = 10^4$	$Re = 10^5$
$\widetilde{S}_{\gamma\ PCD}^{-1}S_{\gamma}$				
$\mathcal{R}_{min}$	0.2062	0.1283	0.1129	0.1992
$\mathcal{R}_{max}$	2.3315	4.2868e+1	4.1574e+2	1.3059e+3
$\mathcal{R}_{max}/\mathcal{R}_{min}$	1.1621e+1	3.3412e+2	3.6824e+3	6.5557e+3
$\mathcal{I}_{max}$	0.2567	1.2106	1.1109e+1	1.2598e+2
$\widetilde{S}_{\gamma\ LSC}^{-1}S_{\gamma}$				
$\mathcal{R}_{min}$	0.2537	0.2530	0.8865	0.5652
$\mathcal{R}_{max}$	2.1509e+1	1.0623e+1	1.0973e+1	1.1309e+2
$\mathcal{R}_{max}/\mathcal{R}_{min}$	8.4782e+1	4.1991e+1	1.2378e+1	2.0009e+2
$\mathcal{I}_{max}$	2.2301e+1	4.6429	4.6264e+1	8.8363e+2
$\widetilde{S}_{\gamma\ SIMPLE}^{-1}S_{\gamma}$				
$\mathcal{R}_{min}$	0.6714	0.4075	0.1949	0.1541
$\mathcal{R}_{max}$	2.9729e+1	9.8786	3.1976	1.4942
$\mathcal{R}_{max}/\mathcal{R}_{min}$	4.4280e+1	2.4241e+1	1.6406e+1	9.6963
$\mathcal{I}_{max}$	5.3308	1.0578	0.1630	0.1755
$\widetilde{S}_{\gamma\ \mathrm{old}}^{-1}S_{\gamma}$				
$\mathcal{R}_{min}$	0.161e-1	0.167e-1	0.3423e-2	0.1315e-3
$\mathcal{R}_{max}$	0.8000	0.9231	0.9524	0.9524
$\mathcal{R}_{max}/\mathcal{R}_{min}$	4.9689e+1	5.5275e+1	2.8011e+2	7.2382e+3
$\mathcal{I}_{max}$	0.1081	0.2458	0.3078	0.3404

Table 15: The optimal Schur complement approximation $\widetilde{S}_{\gamma\ \mathrm{opt}}$ in the modified AL preconditioner on varying classes of evaluations.

class of evaluations	$\widetilde{S}_{\gamma\ \mathrm{opt}}$	mesh independence	problem independence
$Re = 10^2$ and uniform grid	$\widetilde{S}_{\gamma\ \mathrm{old}}$	Yes	Yes
$Re = 10^3$ and uniform grid	$\widetilde{S}_{\gamma\ LSC}$	Yes	Yes
$Re = 10^3$ and stretched grid	$\widetilde{S}_{\gamma\ PCD}$	Yes	Yes
$Re \geq 10^4$ and stretched grid	$\widetilde{S}_{\gamma\ SIMPLE}$	No	Yes

4.6 Comparison between $\mathcal{P}_{MAL}$ and $\mathcal{P}_U$.

To apply the modified AL preconditioner $\mathcal{P}_{MAL}$, one needs to transform the original system (2) to an equivalent one (13) with the coefficient matrix $\mathcal{A}_\gamma$. This transformation consumes additional costs. Furthermore, at each Krylov iteration extra costs arise from the product of $\mathcal{A}_\gamma$ with a Krylov residual vector due to more fill-in in $\mathcal{A}_\gamma$ [17]. In this sense, the heavier complexities of $\mathcal{P}_{MAL}$ could be payed off only by a reduced number of Krylov iterations, compared to the block upper-triangular preconditioner $\mathcal{P}_U$ applied to the original system. In this section, we consider the comparisons between $\mathcal{P}_{MAL}$ and $\mathcal{P}_U$ on the LDC and FP cases at the large Reynolds number $Re = 10^4$ and stretched grid which represent stiff tests on the considered preconditioners.

It is revealed in Section 4.4 that $\widetilde{S}_{\gamma\ SIMPLE}$ turns out to be the most efficient Schur complement approximation for the modified AL preconditioner $\mathcal{P}_{MAL}$ in this class of evaluations. Therefore, the comparison is carried out between $\mathcal{P}_{MAL}$ with $\widetilde{S}_{\gamma\ SIMPLE}$ and $\mathcal{P}_U$ and presented in Table 16. As seen, less iterations are needed when applying $\mathcal{P}_{MAL}$ with $\widetilde{S}_{\gamma\ SIMPLE}$. Considering the LDC case on the finest grid, the application of $\mathcal{P}_{MAL}$ with $\widetilde{S}_{\gamma\ SIMPLE}$ reduces the number of Krylov iterations by a factor about four, seven and two, compared to that by using $\mathcal{P}_U$ with $\widetilde{S}_{PCD}$, $\widetilde{S}_{LSC}$ and $\widetilde{S}_{SIMPLE}$, respectively. On the FP case, a further reduction factor of Krylov iterations is obtained by using $\mathcal{P}_{MAL}$ with $\widetilde{S}_{\gamma\ SIMPLE}$. One direction of future research is to verify whether the reduced number of Krylov iterations could convert to the advantage of $\mathcal{P}_{MAL}$ with $\widetilde{S}_{\gamma\ SIMPLE}$ in terms of the total computational costs.

Table 16: $\mathbf{Re = 10^4}$ and **stretched grid**: the number of GMRES iterations to solve the transformed system with $\mathcal{A}_\gamma$ preconditioned by $\mathcal{P}_{MAL}$ and the number of GMRES iterations to solve the original system with $\mathcal{A}$ preconditioned by $\mathcal{P}_U$.

	$\mathcal{P}_{MAL}$ for $\mathcal{A}_\gamma$	$\mathcal{P}_U$ for $\mathcal{A}$		
	$\widetilde{S}_{\gamma\ SIMPLE}$	$\widetilde{S}_{PCD}$	$\widetilde{S}_{LSC}$	$\widetilde{S}_{SIMPLE}$
LDC case:				
$n = 6$	34(1.e-3)	130	147	83
$n = 7$	45(1.e-3)	246	307	119
$n = 8$	80(2.e-3)	364	560	182
FP case:				
$n = 5$	35(2.e-3)	879	661	62
$n = 6$	53(3.e-3)	1000+	599	122
$n = 7$	83(4.e-3)	1000+	809	229

5 Conclusion and future work

In this paper we introduce three variants based on the new method to approximate the Schur complement for the AL preconditioner. To evaluate the performance, we classify the numerical experiments to four categories according to the Reynolds number and mesh anisotropy. At every class of evaluations we consider different test problems. The optimal Schur complement for every class of tests is determined and given in Table 15. It is seen that the most efficient Schur complement approximation is dependent of the Reynolds number and mesh anisotropy, but problem independent. Furthermore, we find out that, except the experiments at $Re = 10^2$ and uniform grid, the optimal Schur complement approximations on the other three classes of tests are the variants derived from the new method to approximate the Schur complement in the modified AL preconditioner. This demonstrates the advantage of the new approach over the traditional Schur complement approximation.

In this paper we observe that for large Reynolds numbers $Re \geq 10^4$ none of the considered Schur complement approximations can make the modified AL preconditioner independent of the grid size. One planned future research is on the improvement which allows the mesh independence. Another direction of future work is to evaluate whether the advantage of the modified AL preconditioner by the reduced number of Krylov iterations, which is shown in this paper, can convert to the wall-clock time benefit with respect to the preconditioner applied to the original system.

References

[1] R. Becker and M. Braack. A finite element pressure gradient stabilization for the Stokes equations based on local projections. *Calcolo*, 38:173–199, 2001.

[2] M. Benzi, G.H. Golub, and J. Liesen. Numerical solution of saddle point problems. *Acta numerica*, 14:1–137, 2005.

[3] M. Benzi and M.A. Olshanskii. An augmented Lagrangian-based approach to the Oseen problem. *SIAM Journal on Scientific Computing*, 28:2095–2113, 2006.

[4] M. Benzi, M.A. Olshanskii, and Z. Wang. Modified augmented Lagrangian preconditioners for the incompressible Navier-Stokes equations. *International Journal for Numerical Methods in Fluids*, 66:486–508, 2011.

[5] P.B. Bochev, C.R. Dohrmann, and M.D. Gunzburger. Stabilization of low-order mixed finite elements for the Stokes equations. *SIAM Journal on Numerical Analysis*, 44:82–101, 2006.

[6] R. Codina. A stabilized finite element method for generalized stationary incompressible flows. *Computer Methods in Applied Mechanics and Engineering*, 190:2681–2706, 2001.

[7] C.R. Dohrmann and P.B. Bochev. A stabilized finite element method for the Stokes problem based on polynomial pressure projections. *International Journal for Numerical Methods in Fluids*, 46:183–201, 2012.

[8] H. Elman, V.E. Howle, J. Shadid, R. Shuttleworth, and R. Tuminaro. Block preconditioners based on approximate commutators. *SIAM Journal on Scientific Computing*, 27:1651–1668, 2006.

[9] H. Elman, V.E. Howle, J. Shadid, D. Silvester, and R. Tuminaro. Least squares preconditioners for stabilized discretizations of the Navier-Stokes equations. *SIAM Journal on Scientific Computing*, 30:290–311, 2007.

[10] H. Elman and R.Tuminaro. Boundary conditions in approximate commutator preconditioners for the Navier-Stokes equations. *Electronic Transactions on Numerical Analysis*, 35:257–280, 2009.

[11] H. Elman, D. Silvester, and A. Wathen. *Finite elements and fast iterative solvers: with applications in incompressible fluid dynamics*. Oxford University Press, 2014.

[12] J.H. Ferziger and M. Peric. *Computational methods for fluid dynamics*. Springer Science & Business Media, 2012.

[13] L.P. Franca and A. Russo. Approximation of the Stokes problem by residual-free macro bubbles. *Journal of Numerical Mathematics*, 4:265–278, 1996.

[14] A. Greenbaum, V. Pták, and Z. Strakoš. Any nonincreasing convergence curve is possible for GMRES. *SIAM Journal on Matrix Analysis and Applications*, 17:465–469, 1996.

[15] X. He, M. Neytcheva, and S.S. Capizzano. On an augmented Lagrangian-based preconditioning of Oseen type problems. *BIT Numerical Mathematics*, 51:865–888, 2011.

[16] X. He and C. Vuik. Comparison of some preconditioners for the incompressible Navier-Stokes equations. *Numerical Mathematics: Theory, Methods and Applications*, 9:239–261, 2016.

[17] X. He, C. Vuik, and C.M. Klaij. Block-preconditioners for the incompressible Navier-Stokes equations discretized by a finite volume method. *Journal of Numerical Mathematics*, 25:89–105, 2017.

[18] X. He, C. Vuik, and C.M. Klaij. Combining the augmented Lagrangian preconditioner with the SIMPLE Schur complement approximation. *SIAM Journal on Scientific Computing*, 40:A1362–A1385, 2018.

[19] V.E. Howle, J. Schroder, and R.Tuminaro. The effect of boundary conditions within pressure convection-diffusion preconditioners. Technical Report SAND2006-4466, SANDIA, 2006.

[20] T.J.R. Hughes, L.P. Franca, and M. Balestra. A new finite element formulation for computational fluid dynamics: V. circumventing the babuska-brezzi condition: a stable petrov-galerkin formulation of the Stokes problem accommodating equal-order interpolations. *Computer Methods in Applied Mechanics and Engineering*, 59:85–99, 1986.

[21] D. Kay, D. Loghin, and A. Wathen. A preconditioner for the steady-state Navier-Stokes equations. *SIAM Journal on Scientific Computing*, 24:237–256, 2002.

[22] C.M. Klaij. On the stabilization of finite volume methods with co-located variables for incompressible flow. *Journal of Computational Physics*, 297:84–89, 2015.

[23] C.M. Klaij, X. He, and C. Vuik. On the design of block preconditioners for maritime engineering. In M. Visonneau, P. Queutey, and D. Le Touzé, editors, *Proceedings of the Seventh International Conference on Computational Methods in Marine Engineering MARINE*, 2017. May 15–17, Nantes, France.

[24] C.M. Klaij and C. Vuik. SIMPLE-type preconditioners for cell-centered, colocated finite volume discretization of incompressible Reynolds-averaged Navier-Stokes equations. *International Journal for Numerical Methods in Fluids*, 71:830–349, 2013.

[25] C. Li and C. Vuik. Eigenvalue analysis of the SIMPLE preconditioning for incompressible flow. *Numerical Linear Algebra with Applications*, 11:511–523, 2004.

[26] T.F. Miller and F.W. Schmidt. Use of a pressure-weighted interpolation method for the solution of the incompressible Navier-Stokes equations on a nonstaggered grid system. *Numerical Heat Transfer, Part A: Applications*, 14:213–233, 1988.

[27] M.A. Olshanskii and E.E. Tyrtyshnikov. *Iterative methods for linear systems: theory and applications*. SIAM, 2014.

[28] S.V. Patankar. *Numerical heat transfer and fluid flow*. McGraw-Hill, 1980.

[29] J. Pestana and A.J. Wathen. Natural preconditioning and iterative methods for saddle point systems. *SIAM Review*, 57:71–91, 2015.

[30] Y. Saad, V. der Vorst, and A. Henk. Iterative solution of linear systems in the 20th century. *Journal of Computational and Applied Mathematics*, 123:1–33, 2000.

[31] A. Segal, M. ur Rehman, and C. Vuik. Preconditioners for incompressible Navier-Stokes solvers. *Numerical Mathematics: Theory, Methods and Applications*, 3:245–275, 2010.

[32] D. Silvester, H. Elman, D. Kay, and A. Wathen. Efficient preconditioning of the linearized Navier-Stokes equations for incompressible flow. *Journal of Computational and Applied Mathematics*, 128:261–279, 2001.

[33] C. Vuik, A. Saghir, and G.P. Boerstoel. The Krylov accelerated SIMPLE(R) method for flow problems in industrial furnaces. *International Journal for Numerical methods in fluids*, 33:1027–1040, 2000.

[34] P. Wesseling. *Principles of computational fluid dynamics*. Springer Science & Business Media, 2009.